of the reaction amplitude near the nuclear surface for heavy-ion reactions. Application of the EFR DWBA showed excellent agreement with experimental results provided the Coulomb interaction in the perturbing potential is properly taken into account. Of course, in principle, the very small charge-dependent nuclear interactions will also play a role in these comparisons. But the current levels of sophistication of both theory and experiment are not sufficient to warrant these considerations in our present results. Since the choice was made such that a number of ambiguities present in usual direct-reaction studies were minimized, this may be one of the most accurate checks of the DWBA analyses applied to heavy-ion reactions. Extension of such studies to heavier nuclei and also to multinucleon transfers should be fruitful since there the Coulomb effects are expected to be even more important.

We would like to express our appreciation to K. I. Kubo for some useful discussions. A. Bachher, C. Towsley, M. Hamm, and R. Hanus are thanked for their help at various stages of this investigation.

*Work supported in part by the National Science Foundation.

†Permanent address: Physikalisches Institut der Universität Erlangen-Nurnberg, Erlangen, W. Germany.

[1]R. E. Tribble, to be published.

[2]K. O. Groeneveld *et al.*, Phys. Rev. Lett. 27, 1806 (1971).

[3]S. Barshay and G. M. Temmer, Phys. Rev. Lett. 12, 728 (1964); also see D. Robson and A. Richter, Ann. Phys. (N.Y.) 63, 261 (1971).

[4]H. Voit *et al.*, Phys. Lett 58B, 152 (1975).

[5]K. G. Nair *et al.*, Phys. Rev. C 12, 1575 (1975).

[6]K. G. Nair *et al.*, Phys. Rev. C 8, 1129 (1973), and references therein; W. Tobocman *et al.*, Nucl. Phys. A205, 193 (1973).

[7]R. M. DeVries, G. R. Satchler, and J. G. Cramer, Phys. Rev. Lett. 32, 1377 (1974).

Multiphoton Ionization Spectroscopy of High-Lying, Even-Parity States in Calcium*

P. Esherick, J. A. Armstrong, R. W. Dreyfus, and J. J. Wynne
IBM Thomas J. Watson Research Center, Yorktown Heights, New York 10598

(Received 4 December 1975)

Strong ionization signals have been observed in Ca following two-photon absorption to the bound, even-parity $J=0$ and $J=2$ states. Using known Ca absorption lines for calibration, 72 new states have been classified, and their energies have been determined to ± 0.1 cm^{-1}. The new $J=0$ states have a constant quantum defect, whereas the $J=2$ states do not.

Two-photon laser spectroscopy has had great impact on the study of excited atomic and molecular states.[1-4] We have observed strong ionization signals following two-photon absorption of light to 72 previously unknown even-parity $J=0$ and $J=2$ states of Ca. A typical multiphoton ionization spectrum, shown in Fig. 1, illustrates the sensitivity and resolving power of this technique. We have found and identified the $4sns\ ^1S_0$ states from $n=13$ to 30. We have also found 54 $J=2$ states which we have identified as $^1D_2$. The $4snd\ ^1D_2$ series is strongly perturbed by interactions with the $3d5s$ and the $(3d)^2$ $J=2$ levels; this has prevented workers using conventional emission spectroscopy[5] from clearly identifying the "$4snd$" $^1D_2$ series for $n>7$.

The known[6] $4snp\ ^1P_1^\circ$ states converge to the same limit and therefore are as densely spaced as the $4sns\ ^1S_0$ and "$4snd$" $^1D_2$ states. By frequency doubling the laser and using linear absorption to the $4snp\ ^1P_1^\circ$ levels to provide a series of calibration points, the energies of the newly identified states have been determined to ± 0.1 cm^{-1}.

The experimental apparatus consisted of a nitrogen-laser-pumped dye laser,[7] Ca vapor in a heated cylindrical pipe, and an ionization probe. The laser had a linewidth of 0.5 cm^{-1}, a pulse width of ~10 nsec, and a power of 10–50 kW over the range 4025–4325 Å. The beam was focused into the calcium pipe with intensities, I_L, up to 10^8 W/cm^2. The pipe was heated from 600 to 800 °C, yielding Ca pressures, P_{Ca}, from ~0.015 to 1.0 Torr. Diffusion of the Ca vapor to the cold ends of the pipe was prevented by buffer gas (Ne or Kr) at pressures, P_b, from 5 to 50 Torr. The ionization probe was a tungsten wire (2 mm diam) which extended axially into the hot zone of the Ca pipe. This probe was held at a negative potential,

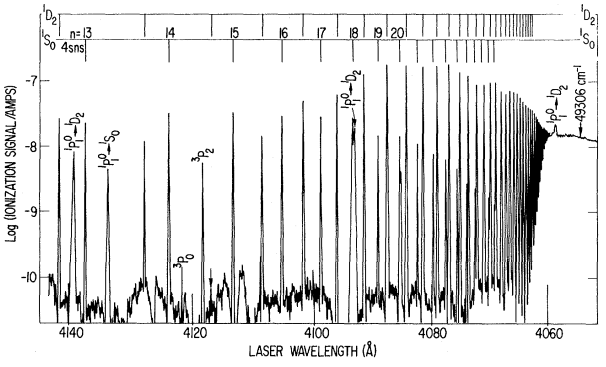

FIG. 1. Two-photon spectrum of $^1S_0$ and $^1D_2$ states converging on the ionization limit at 49 306 cm^{-1}. Experimental conditions are $I_L \simeq 10^7$ W/cm^2 (linearly polarized), $P_{Ca} = 0.1$ Torr, $P_{Kr} = 10$ Torr, and $V \leq 1.0$ V. Two-photon transitions to $^3P_0$ and $^3P_2$ and one-photon transitions from $4s4p\ ^1P_1^\circ$ are indicated.

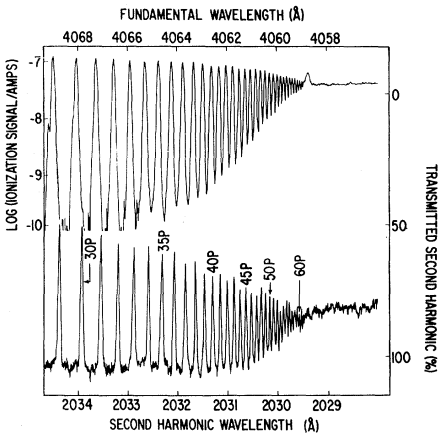

FIG. 2. Simultaneous recording of high-resolution multiphoton-ionization signal (top) and single-photon absorption of the second harmonic (bottom). The shoulders on the two longest-wavelength ionization peaks are the $4s29s\ ^1S_0$ and $4s30s\ ^1S_0$ resonances.

V, with respect to the (19 mm i.d.) tantalum lining of the pipe. No Stark shifts were observed for dc fields <3 V/cm and laser intensities <3 $\times 10^8$ W/cm^2. The probe was capacitively coupled to a box-car integrator; the signal was then logarithmically amplified and recorded as a function of laser wavelength. The $4snp\ ^1P_1^\circ$ wavelength calibrations were simultaneously recorded on the same chart. This was done by measuring the transmission of the second harmonic of the laser (generated in a nonphasematched ammonium-dihydrogen-phosphate crystal) through a second pipe containing <1 Torr of Ca vapor. Buffer-gas pressures were the same in both pipes during wavelength calibration. A portion of a typical spectrum is shown in Fig. 2.

The ionization spectra (Fig. 1) show two types of peaks: (a) narrow peaks with strengths independent of P_b, and (b) broader peaks, with strengths strongly affected by P_b, which essentially disappear for $P_b < 5$ Torr. The latter peaks occur when the laser is tuned to single-photon transitions from $4s4p\ ^1P_1^\circ$ to the even-parity states. The $4s4p\ ^1P_1^\circ$ state is populated by laser absorption in the wings of the Ca-buffer collision-broadened line profile.

The narrow peaks occur when the laser is tuned to half the energy separation between the ground state and even-parity states below the ionization limit. The strength of the narrow peaks is proportional to I_L^2 over three orders of magnitude change in signal strength, up to peak currents of ~1 μA (10^{-9} C in ~1 msec). At higher currents, space-charge and/or recombination effects cause deviations from this behavior.

The signals from the narrow peaks and from the continuum above the ionization limit show identical dependence on the parameters, I_L, P_{Ca}, P_b, and V, as well as identical time behavior. This evidence suggests that the ionizing step from the high-lying bound state to the continuum occurs with unit probability. We are as yet unable to determine if this step is because of photoionization, Stark ionization,[8] or collisions.

A major division of the narrow peaks into two sets is possible. One set is >200 times stronger with linearly polarized light than with circularly polarized light and defines a Rydberg series. Four peaks, at lower energies, coincide with the known[5] $4sns\ ^1S_0$ levels for $n = 9$–12, which therefore assigns this set to the $4sns\ ^1S_0$ series. The remaining narrow peaks are ~$\frac{3}{2}$ times stronger with circularly polarized light than with linearly polarized light. This ratio is consistent with the dependence calculated from angular momentum selection rules for a two-photon transition from a $J = 0$ to a $J = 2$ state. The convergence of these peaks to the $4s\ ^2S_{1/2}$ ionization limit suggests that most of them belong to the "$4snd$" $^1D_2$ series.

Our term values for the $J = 0$ and $J = 2$ states are presented in Table I. To obtain these data, each recorded spectrum was calibrated by least-squares fitting[9] our observed positions of the $4snp\ ^1P_1^\circ$ absorptions with the tabulated wavelengths.[6] To minimize systematic errors due to pressure shifts, the same buffer gas was used at the same pressure in each pipe. To minimize Stark shifts, data were taken with dc fields <1

Energy (cm^{-1})	ν_S	Label	
46836.0 ±0.4	6.665 ± 0.001	$^1S_0$	4s9s
47436.8 ±0.4	7.662 ± 0.001	$^1S_0$	4s10s
47844.4 ±0.4	8.665 ± 0.001	$^1S_0$	4s11s
48131.2 ±0.4	9.665 ± 0.002	$^1S_0$	4s12s
48339.7 ±0.5	10.656 ± 0.003	$^1S_0$	4s13s
48499.1 ±0.3	11.662 ± 0.002	$^1S_0$	4s14s
48524.4 ±0.2	11.849 ± 0.002	$^3P_0$	$(3d)^2$ a
48621.9 ±0.2	12.665 ± 0.002	$^1S_0$	4s15s
48717.78 ±0.09	13.659 ± 0.001	$^1S_0$	4s16s
48795.57 ±0.07	14.663 ± 0.001	$^1S_0$	4s17s
48858.35 ±0.06	15.657 ± 0.001	$^1S_0$	4s18s
48910.82 ±0.07	16.664 ± 0.001	$^1S_0$	4s19s
48954.01 ±0.05	17.657 ± 0.001	$^1S_0$	4s20s
48990.86 ±0.08	18.661 ± 0.002	$^1S_0$	4s21s
49021.99 ±0.08	19.657 ± 0.003	$^1S_0$	4s22s
49048.97 ±0.06	20.663 ± 0.003	$^1S_0$	4s23s
49072.04 ±0.05	21.658 ± 0.002	$^1S_0$	4s24s
49092.23 ±0.05	22.658 ± 0.003	$^1S_0$	4s25s
49109.95 ±0.06	23.659 ± 0.004	$^1S_0$	4s26s
49125.54 ±0.05	24.660 ± 0.003	$^1S_0$	4s27s
49139.39 ±0.05	25.664 ± 0.004	$^1S_0$	4s28s
49151.66 ±0.07	26.666 ± 0.006	$^1S_0$	4s29s
49162.6 ±0.1	27.661 ± 0.010	$^1S_0$	4s30s
46950.2 ±0.4	6.825 ± 0.001	$^1D_2$	
47449.4 ±0.4	7.688 ± 0.001	$^1D_2$	$(3d)^2$ a
47466.4 ±0.4	7.724 ± 0.001	$^3D_2$	3d5s a
47757.9 ±0.4	8.419 ± 0.001	$^3D_2$	4s9d a
47812.6 ±0.4	8.572 ± 0.001	$^1D_2$	
48083.4 ±0.4	9.474 ± 0.002	$^1D_2$	3d5s a
48290.1 ±0.3	10.393 ± 0.001	$^1D_2$	
48433.4 ±0.2	11.214 ± 0.002	$^3D_2$	4s12d a
48451.1 ±0.3	11.329 ± 0.002	$^1D_2$	
48563.7 ±0.2	12.159 ± 0.001	$^3P_2$	$(3d)^2$ a
48569.4 ±0.2	12.206 ± 0.002	$^3D_2$	4s13d a
48578.5 ±0.4	12.282 ± 0.004	$^1D_2$	
48675.7 ±0.2	13.195 ± 0.002	$^3D_2$	4s14d a
48678.6 ±0.2	13.225 ± 0.002	$^1D_2$	
48760.25 ± 0.06	14.180 ± 0.001	$^1D_2$	
48827.02 ± 0.05	15.136 ± 0.001	$^1D_2$	
48882.34 ± 0.05	16.094 ± 0.001	$^1D_2$	
48928.87 ± 0.07	17.058 ± 0.001	$^1D_2$	
48968.26 ± 0.05	18.026 ± 0.001	$^1D_2$	
49001.70 ± 0.06	18.990 ± 0.002	$^1D_2$	
49030.58 ± 0.07	19.961 ± 0.003	$^1D_2$	
49055.78 ± 0.07	20.942 ± 0.003	$^1D_2$	
49077.48 ± 0.06	21.914 ± 0.003	$^1D_2$	
49096.63 ± 0.08	22.894 ± 0.004	$^1D_2$	
49113.47 ± 0.07	23.874 ± 0.004	$^1D_2$	
49128.38 ± 0.05	24.857 ± 0.003	$^1D_2$	
49141.77 ± 0.07	25.850 ± 0.005	$^1D_2$	
49153.54 ± 0.05	26.830 ± 0.004	$^1D_2$	
49164.34 ± 0.05	27.833 ± 0.005	$^1D_2$	
49173.84 ± 0.07	28.816 ± 0.008	$^1D_2$	
49182.50 ± 0.05	29.810 ± 0.006	$^1D_2$	
49190.32 ± 0.05	30.801 ± 0.007	$^1D_2$	
49197.38 ± 0.05	31.786 ± 0.007	$^1D_2$	
49203.88 ± 0.05	32.782 ± 0.008	$^1D_2$	
49209.75 ± 0.05	33.767 ± 0.009	$^1D_2$	
49215.18 ± 0.05	34.76 ± 0.01	$^1D_2$	
49220.18 ± 0.05	35.76 ± 0.01	$^1D_2$	
49224.75 ± 0.05	36.75 ± 0.01	$^1D_2$	
49229.02 ± 0.05	37.76 ± 0.01	$^1D_2$	
49232.92 ± 0.05	38.75 ± 0.01	$^1D_2$	
49236.51 ± 0.05	39.74 ± 0.01	$^1D_2$	
49239.83 ± 0.05	40.73 ± 0.02	$^1D_2$	
49243.06 ± 0.05	41.76 ± 0.02	$^1D_2$	
49245.97 ± 0.05	42.76 ± 0.02	$^1D_2$	
49248.64 ± 0.05	43.74 ± 0.02	$^1D_2$	
49251.20 ± 0.05	44.75 ± 0.02	$^1D_2$	
49253.52 ± 0.05	45.73 ± 0.02	$^1D_2$	
49255.78 ± 0.05	46.75 ± 0.02	$^1D_2$	
49257.76 ± 0.05	47.70 ± 0.02	$^1D_2$	
49259.76 ± 0.05	48.72 ± 0.03	$^1D_2$	
49261.57 ± 0.05	49.70 ± 0.03	$^1D_2$	
49263.29 ± 0.05	50.69 ± 0.03	$^1D_2$	
49264.98 ± 0.05	51.73 ± 0.03	$^1D_2$	
49266.51 ± 0.05	52.72 ± 0.03	$^1D_2$	
49267.92 ± 0.05	53.69 ± 0.04	$^1D_2$	
49269.24 ± 0.05	54.64 ± 0.04	$^1D_2$	
49270.69 ± 0.05	55.75 ± 0.04	$^1D_2$	
49271.83 ± 0.05	56.68 ± 0.04	$^1D_2$	
49272.87 ± 0.07	57.56 ± 0.06	$^1D_2$	
49274.0 ± 0.1	58.54 ± 0.1	$^1D_2$	
49275.0 ± 0.1	59.5 ± 0.1	$^1D_2$	
49275.9 ± 0.1	60.4 ± 0.1	$^1D_2$	

[a] Configuration assigned by Ref. 5.

TABLE I. Observed $J=0$ and $J=2$ states. Listed errors are standard deviations reflecting relative accuracy; systematic error is believed to be $\leq \pm 0.1$ cm^{-1}.

V/cm. With ~45 $^1P_1^\circ$ calibration lines on a spectrum, the rms deviation between Ref. 6 and our fitted results was 0.12 cm^{-1}. By averaging five spectra, the rms error was reduced to 0.05 cm^{-1}. Variations in peak positions using alternatively Ne or Kr at $P_b = 10$ Torr were within experimental error. (With unequal pressures in the two pipes, we measured pressure shifts of -0.8 cm^{-1}/100 Torr Kr and $< +0.02$ cm^{-1}/100 Torr Ne. Pressure shifts from Ca were not observable, even at pressures 10 times higher than those used for wavelength calibration.) Systematic errors are believed to be less than 0.1 cm^{-1}.

The spectra show a striking decrease in signal intensity of the $J=2$ peaks around the level at 48 578.5 cm^{-1}. The signal from this level, which is orders of magnitude smaller than that from neighboring $J=2$ levels, is observed only in high-resolution scans.

In Fig. 3 we give a Lu-Fano plot[10] of the experimental data for the $J=2$ states. For each term, an effective quantum number, ν, is determined both for a series converging to Ca II $^2S_{1/2}(\nu_S)$ (49 305.99 cm^{-1})[6] and for one to Ca II $^2D_{3/2,5/2}(\nu_S)$ (63 016.93 cm^{-1}). This figure plots the nonintegral parts of $(-\nu_S)$ versus ν_D. The solid lines and the dashed line are from a multichannel[10] theoretical fit to our $^1D_2$ data and to the $^3D_2$ states. Known levels and theoretical channel

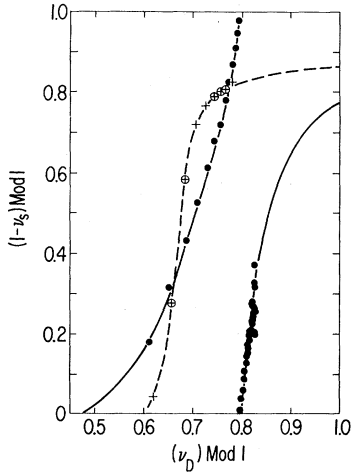

FIG. 3. Multichannel quantum-defect plot of $J=2$ states. The symbols are ● for $^1D_2$, + for $^3D_2$ (Ref. 5), and ⊕ for $^3D_2$ observed in this experiment.

curves for small values of n have been omitted, but will be included in a subsequent publication.[11] In the regions where the triplet and singlet channels cross there is a slight mixing of the channels, which gives rise to the multiphoton ionization signals seen from the triplet states (Table I). The strong interaction between the $4snd\,^1D_2$, $3d5s\,^1D_2$, and $3d^2\,^1D_2$ configurations is clearly seen in the substantial deviation of the channels from the horizontal or vertical lines which would be predicted for Ca in the absence of such interactions. It is obvious that assigning unmixed configurations to particular peaks is highly suspect for $^1D_2$ states. In fact, the multichannel analysis[11] shows that none of the newly observed $^1D_2$ states contains more than a few percent admixture of $3d5s$ or $3d^2$. By contrast, the quantum defects for the $4sns\,^1S_0$ states (Table I) show no evidence of perturbation by the (as yet unobserved) $3d^2\,^1S_0$ state.

We gratefully acknowledge useful discussions with Dr. P. P. Sorokin and the technical assistance of Mr. L. H. Manganaro.

*Supported in part by the U. S. Army Research Office.

[1]F. Biraben, B. Cagnac, and G. Grynberg, Phys. Rev. Lett. 32, 643 (1974); M. D. Levenson and N. Bloembergen, Phys. Rev. Lett. 32, 645 (1974).

[2]D. Popescu, C. B. Collins, B. W. Johnson, and I. Popescu, Phys. Rev. A 9, 1182 (1974).

[3]R. M. Hochstrasser, H. N. Sung, and J. E. Wessel, J. Chem. Phys. Lett. 24, 7 (1974).

[4]P. M. Johnson, J. Chem. Phys. 62, 4562 (1975).

[5]G. Risberg, Ark. Fys. 37, 231 (1968).

[6]C. M. Brown, S. G. Tilford, and M. L. Ginter, J. Opt. Soc. Am. 63, 1454 (1973).

[7]T. W. Hänsch, Appl. Opt. 11, 895 (1972).

[8]T. W. Ducas, M. G. Littman, R. R. Freeman, and D. Kleppner, Phys. Rev. Lett. 35, 366 (1975).

[9]P. R. Bevington, *Data Reduction and Error Analysis for the Physical Sciences* (McGraw-Hill, New York, 1969), Chap. 11.

[10]U. Fano, J. Opt. Soc. Am. 65, 979 (1975), and refercences cited therein.

[11]J. A. Armstrong, P. Esherick, and J. J. Wynne, to be published.

Optical Potential for He(2^1S) + Ar from High-Resolution Differential Scattering Experiments

B. Brutschy, H. Haberland, H. Morgner, and K. Schmidt
Fakultät für Physik der Universität Freiburg, 78 Freiburg im Breisgau, West Germany
(Received 20 January 1976)

The real and imaginary parts of the interaction potential of metastable He(2^1S) with argon have been accurately determined from high-resolution differential scattering experiments. The real part of the potential shows an unexpected structure with two minima, while the imaginary part is monotonic, but cannot be expressed by a single exponential.

If a metastable helium atom (He*) collides with a ground-state argon atom it can either be scattered elastically or it can ionize the argon because its excitation energy is more than 4 eV higher than the ionization potential of argon. This inelastic process, called Penning ionization, has been extensively studied in recent years.[1] The ionization causes a loss of flux from the incident beam. When inelastic channels are open a scattering process can be phenomenologically described by a complex potential $W(R)=V(R)-i\Gamma(R)/2$, where $\Gamma(R)$ is usually called the width of the potential. Complex or optical potentials which have been used extensively in nuclear physics[2] have also been used in the analyses of molecular-beam experiments with metastable helium[3,4] and with chemically reactive molecules.[5] If the optical potential is defined rigorously it becomes energy dependent and nonlocal.[2,5] In the case of scattering metastable helium from atoms, a local Born-Oppenheimer–type of approximation will probably be rather good, because the loss from the incoming channel is due to an electronic transition which is very fast compared to the heavy-particle motion.

A large number of experiments have been performed to determine some of the properties of the He*-Ar system. Measurements have been made of the energy dependence of the total elastic cross section, of quenching and ionization rate constants and cross sections, and of the velocity dependence of the Penning electron energy and angular distributions.[1] The angular distributions of the resulting Ar^+ have also been measured.[6] The theory has been developed mainly by Nakamura[7] and Miller.[8]